JOURNAL OF COMPUTATIONAL PHYSICS 106, 215–233 (1993)

Numerical Computation of Two-Dimensional Unsteady Detonation Waves in High Energy Solids*

J. F. CLARKE, S. KARNI,† J. J. QUIRK,‡ P. L. ROE,§ L. G. SIMMONDS, AND E. F. TORO

College of Aeronautics, Cranfield Institute of Technology, Cranfield, Bedford MK43 OAL, United Kingdom

Received December 7, 1990

We are concerned with theoretical modelling of unsteady, two-dimensional detonation waves in high energy solids. A mathematical model and a numerical method to solve the associated hyperbolic system of equations are presented. The model consists of the Euler equations augmented by extra conservation laws and source terms to account for chemical reaction and tracking of materials. Both the thermodynamics and the chemistry are treated in a simple way. Using a detonation analogue due to Fickett, we test several numerical methods and assess their performance in modelling the essential features of detonation waves. The numerical method selected for the full model is an extension of the conservative, shock capturing technique of Roe, together with an adaptive mesh refinement procedure that allows the resolution of fine features such as reaction zones. Results for some typical tests problems are presented.

1. INTRODUCTION

This paper is concerned with numerical simulation of detonation waves in high-energy solids (chemical explosives). A detonation wave is a shock wave that precedes and is driven by a zone of chemical reaction. The passage of the shock wave through the explosive initiates chemical activity which in turn generates chemical-energy heat release that sustains the propagation of the shock wave. The recent book by Fickett and Davies [11] is a useful compendium of information about the detonation phenomenon which makes it clear that such waves are physico-chemical phenomena of extreme features. They travel at typical speeds of 8000 m/s; the reaction zone has a typical width of 10^{-4} m and typical times to complete the reaction are of the order of 10^{-6} s; typical peak pressure values are 50 to 100 giga Pascals.

Studies aimed at understanding the detonation phenomenon have relied heavily on experimental work, but this approach is always expensive, often dangerous, and sometimes impossible. Theoretical studies, on the other hand, have their own difficulties.

If the explosive is a heterogeneous material, which in practice is most likely, then multi-phase flow models must be adopted. This can lead to ill-posed mathematical problems [25, 12]. Single-phase flow models are reasonably well understood but might not furnish accurate descriptions of reality. The thermodynamic behaviour of high explosive material in the construction of realistic equations of state is an active area of current research. Knowledge of the character and speed of the chemical change is also far from complete and requires a continuing research effort in its own right. For almost any moderately realistic model for the fluid dynamics, the thermodynamics, and the chemistry of the detonation problem, the complexity of the equations will be such that analytical tools for their solution will almost certainly be ruled out. There is a very impressive body of work based on analytical approaches (e.g., [3, 26]), but this is strictly for the special case of steady detonations.

In recent years, numerical methods have become a useful alternative method of solution, which, if carefully used, can assist in the understanding of the behaviour of detonations. However, there are some specific problems associated with the numerical simulation of these phenomena. One problem is the accurate resolution of shock waves. Detonation waves have very strong shocks. Typical pressure ratios across the shock are of the order of 10^6. Naive numerical methods must be discarded immediately if the leading shock wave is to be accurately resolved [5]. The reaction zone attached to the shock presents another numerical difficulty. It must be resolved accurately, for it is the very mechanism that sustains the leading shock and thus the detonation itself. Given the small width of the reaction zone, accuracy in its resolution requires very fine meshes. For models of two-

* This work was sponsored by AWE, Aldermaston.

† Present address: Department of Mathematics, University of Michigan, Ann Arbor, MI 48109.

‡ Present address: Institute for Computer Applications in Science and Engineering, NASA Langley Research Center, Hampton, Virginia 23665.

§ Present address: Department of Aerospace Engineering, University of Michigan, Ann Arbor, MI 48109.

0021-9991/93 $5.00

581/106/2-2

or three-dimensional behaviour this poses a virtually impossible computing task if regular static meshes are used.

Another numerical problem occurs in the treatment of the source terms that must be present in the conservation equations. Modern numerical methods based on the solution of local Riemann problems have proved very successful in conventional unreactive compressible fluid dynamics [23]. The presence of source terms in the governing balance equations presents new numerical problems for which the theory is still tentative [24, 27]. The problem is made even more serious by the kind of reactive flow problem posed by detonation waves. The time scale associated with the flow (sometimes called hydrodynamic time) can be several orders of magnitude larger than typical times associated with the chemical reactions involved. A consequence is that the source terms governing the release of chemical energy can lead to stiff systems of equations. For example, if time-operator splitting is used to deal with the source terms then at each time step one must solve a stiff system of ordinary differential equations. Leveque and Yee [17] have clearly demonstrated the need for caution in this respect, although we have not experienced their problems with the simple source terms that we have used during the present work.

A numerical problem that is linked to the modelling problem is that of distinguishing, without ambiguity, between the various materials that may be involved (e.g., unreacted solid explosive, metal container or casing, combustion products, ambient material). One approach, that is attractive in its simplicity, augments the system of conservation laws and adapts the shock-capturing philosophy to find material interfaces [20]. There are still, however, unresolved problems with this approach.

In this paper we adopt a simplified mathematical model consisting of the unsteady two-dimensional Euler equations of gas dynamics with an ideal equation of state suitably augmented to represent the chemistry. A very simple reaction rate equation is chosen. The complete model and underlying assumptions are described in Section 2, in Section 3 we justify the choice of our numerical method. This is based on extensive numerical experimentation of a detonation analogue due to Fickett [10]. In Section 4 we describe the numerical method, which is an extension of one originally due to Roe [22]. In Section 5 we introduce a time-dependent adaptive gridding procedure to resolve fine features such as shock waves and reaction zones. Numerical tests are presented in Section 6.

2. MATHEMATICAL MODEL

The governing equations are the Euler equations, describing inviscid compressible flow with the chemical reaction added. The model allows for a single chemical reaction to take place, during which the unreacted material A changes into the reaction product B. The chemical reaction is modelled by a reaction progress variable λ, which denotes the mass fraction of material B, and accordingly assumes values between $\lambda = 0$ (unreacted; pure A) and $\lambda = 1$ (reaction complete; pure B). Using ρ to denote the density, u and v the velocity components, p the pressure, and E the total energy, the equations read

$$(\rho)_t + (\rho u)_x + (\rho v)_y = 0 \tag{1a}$$

$$(\rho u)_t + (\rho u^2 + p)_x + (\rho uv)_y = 0 \tag{1b}$$

$$(\rho v)_t + (\rho uv)_x + (\rho v^2 + p)_y = 0 \tag{1c}$$

$$(E)_t + (uE + up)_x + (vE + vp)_y = 0 \tag{1d}$$

$$(\lambda)_t + u(\lambda)_x + v(\lambda)_y = r. \tag{1e}$$

The first four equations in (1) express the usual conservation of mass, two momenta components, and energy. The fifth is a rate equation, describing the rate of production of reacted material B along particle paths. To complete, the equation of state and the reaction rate must be related to the thermodynamic and chemical state of the material; for example,

$$p = p(\rho, e, \lambda) \tag{1f}$$

$$r = r(\rho, e, \lambda), \tag{1g}$$

with e being the internal energy per unit mass. Various choices are possible here for the equation of state. In this model, we use the equation of state for ideal gases, which in the reactive case allows for heat release due to chemical activity and reads

$$e = \frac{p}{\rho(\gamma - 1)} - \lambda Q. \tag{2}$$

Here, γ is the usual specific heat ratio and Q is the heat release per unit mass of the material. The total energy E is related to the internal energy in the usual way, $E = \rho e + \frac{1}{2}\rho(u^2 + v^2)$. Although based on the ideal gas assumption, Eq. (2) still makes a good approximation for modelling the chemical activity in solid explosives, with γ constant taken as $\gamma \cong 3$ (see [10]). Other, more realistic, choices include the JWL equation of state (e.g., [11]).

In general, the reaction rate r may depend on λ as well as on the density ρ and the internal energy e. Here, we adopt

the simple reaction rate proposed by Fickett [10], which does not depend explicitly on the flow variables,

$$r=\frac{2}{T_R}(1-\lambda)^{1/2}, \tag{3}$$

where T_R is a typical time associated with the reaction. This choice of reaction rate has the property that the reaction along particle paths is complete within a finite time T_R, yielding reaction zones of well-determined finite widths.

To solve problems involving more than one chemical material with possibly different heat release constants Q_j, the model (1) has to be extended. In particular, it should be possible to identify without ambiguities each material during the course of calculation and so choose the value of Q_j accordingly. One such example is the rate-stick problem, where chemical reaction is taking place in a reactant encased within a non-reacting material (e.g., air or a metal container). Misidentifying the material may, for example, allow chemical reaction to take place in a non-reactive medium. This may lead to incorrect energy balance via a wrong amount of energy release during the burning process. To avoid ambiguities, one should be able to identify and follow the propagating material interfaces. For this purpose, we adopt an interface capturing technique, recently proposed by Osher and Sethian [20] which is capable of handling complicated topological merging and breaking of moving subdomains in quite a natural way. We make Q a piecewise constant function $Q=Q(x, y, t)$, representing the local heat release constant. Being passively carried with the fluid, $Q(x, y, t)$ has an initially known distribution and its evolution is governed by the advection equation

$$Q_t+uQ_x+vQ_y=0, \tag{4}$$

expressing that Q remains constant along particle paths. Initial discontinuities in Q are later represented by smeared, rapidly varying, Q profiles. The location of the interface between material A with Q_A and material B with Q_B is given by the interpolated contour $Q(x, y, t)=\frac{1}{2}(Q_A+Q_B)$.

For computational convenience, we have used (1a) to express the equations for both λ and Q in conservation form (the former with a source term). The complete model of unsteady compressible reactive Euler equations in two space dimensions is given by

$$\mathbf{W}_t+\mathbf{F}(\mathbf{W})_x+\mathbf{G}(\mathbf{W})_y=\mathbf{S}(\mathbf{W}) \tag{5}$$

$$\mathbf{W}=\begin{pmatrix}\rho\\ \rho u\\ \rho v\\ E\\ \rho\lambda\\ \rho Q\end{pmatrix},\quad \mathbf{F}=\begin{pmatrix}\rho u\\ \rho u^2+p\\ \rho uv\\ uE+up\\ \rho u\lambda\\ \rho uQ\end{pmatrix},$$

$$\mathbf{G}=\begin{pmatrix}\rho v\\ \rho uv\\ \rho v^2+p\\ vE+vp\\ \rho v\lambda\\ \rho vQ\end{pmatrix},\quad \mathbf{S}=\begin{pmatrix}0\\ 0\\ 0\\ 0\\ \rho r\\ 0\end{pmatrix}$$

$$p=(\gamma-1)[E-\tfrac{1}{2}\rho(u^2+v^2)+\rho\lambda Q]$$

$$r=\frac{2}{T_R}(1-\lambda)^{1/2}.$$

An "ignition criterion" is used to decide whether reaction is initiated, which is based on (a) local pressure level and (b) heat release variable. The combined criterion takes the form

$p>p_{\text{act}}; Q>Q_{\text{act}}$	sources activated
otherwise	sources not activated.

The first condition ensures that reaction is initiated only if local pressure is greater than a given threshold pressure p_{act}, the choice of which is dictated by chemical considerations. The second distinguishes between reactive and non-reactive flow regions. Setting Q_{act} at $Q_{\text{act}}=Q^*/2$, Q^* being the heat release constant of the reactive material, locates the interface between reactive and non-reactive materials and ensures that reaction takes place only in the reactive part of the flow.

For later reference, the Jacobian matrices of (5) are given by

$$A=\begin{pmatrix}0 & 1 & 0 & 0 & 0 & 0\\ \frac{(\gamma-1)}{2}b-u^2 & (3-\gamma)u & -(\gamma-1)v & \gamma-1 & (\gamma-1)Q & (\gamma-1)\lambda\\ -uv & v & u & 0 & 0 & 0\\ -u\left(H-\frac{(\gamma-1)}{2}b\right) & H-(\gamma-1)u^2 & -(\gamma-1)uv & \gamma u & (\gamma-1)Qu & (\gamma-1)\lambda u\\ -u\lambda & \lambda & 0 & 0 & u & 0\\ -uQ & Q & 0 & 0 & 0 & u\end{pmatrix} \tag{6a}$$

$$B=\begin{pmatrix} 0 & 0 & 1 & 0 & 0 & 0 \\ -uv & v & u & 0 & 0 & 0 \\ \frac{(\gamma-1)}{2}b-v^2 & -(\gamma-1)u & (3-\gamma)v & \gamma-1 & (\gamma-1)Q & (\gamma-1)\lambda \\ -u\left(H-\frac{(\gamma-1)}{2}b\right) & -(\gamma-1)uv & H-(\gamma-1)v^2 & \gamma v & (\gamma-1)Qu & (\gamma-1)\lambda u \\ -v\lambda & \lambda & 0 & 0 & v & 0 \\ -vQ & Q & 0 & 0 & 0 & v \end{pmatrix} \tag{6b}$$

with $|q|=\sqrt{u^2+v^2}$ the flow velocity, $b=q^2-2\lambda Q$, and H the specific enthalpy function

$$H=\frac{E+p}{\rho}.$$

The speed of sound is given by

$$a^2=\frac{\gamma p}{\rho}=(\gamma-1)\left[H-\frac{1}{2}q^2+\lambda Q\right].$$

The Jacobian matrix $A(\mathbf{W})$ admits six characteristic speeds (counted with multiplicity), which are given by the diagonal matrix

$$\Lambda=\text{diag}(u-a,\ u,\ u,\ u,\ u,\ u+a) \tag{7}$$

and the corresponding matrix of right eigenvectors is

$$R(\mathbf{W})=\begin{pmatrix} 1 & 1 & 0 & 0 & 0 & 1 \\ u-a & u & 0 & 0 & 0 & u+a \\ v & v & 1 & 0 & 0 & v \\ H-ua & \frac{1}{2}q^2 & v & -Q & -\lambda & H+ua \\ \lambda & \frac{1}{2}\lambda & 0 & 1 & 0 & \lambda \\ Q & \frac{1}{2}Q & 0 & 0 & 1 & Q \end{pmatrix}. \tag{8}$$

The eigenspace associated with the four equal eigenvalues can, of course, be represented by an arbitrary set of basis vectors, but some sets have more physical meaning than others. Columns 2 to 5 of (8) represent respectively disturbances associated with an entropy wave, a shear wave, a material interface, and a reaction front. The eigenstructure of the Jacobian matrix B has a similar form.

3. THE CHOICE OF NUMERICAL SCHEMES

Using Eqs. (5), we wish to model detonation waves. These are fast moving strong shock fronts of negligible thickness and spiky profiles, followed by a narrow reaction zone, inside which the flow relaxes from its frozen post-shock state to its new equilibrium state. Accurate resolution of flow details inside the reaction zone is extremely important, for it is the heat released during the reaction that sustains the propagation of the leading shock. A suitable numerical technique should thus be capable of capturing cleanly strong spiky shocks and of accurately resolving the flow structure in the narrow reaction zone that follows. A variety of modern methods exist, which have produced very impressive results when applied to chemically non-reactive gas. Their adequacy for problems which are further complicated by chemical activity is not obvious and requires further study.

Broadly speaking, we have looked into two main classes of techniques: (a) deterministic high-resolution schemes and (b) random-choice methods. We have also studied hybrid schemes in an attempt to combine the merits of both classes. Schemes in the first category are essentially shock-capturing algorithms, which do not require a special procedure to resolve disctontinuous flow features. As a consequence, flow discontinuities and sharp corners tend to be smeared over several mesh intervals. The schemes having reached a high degree of sophistication, the smearing can be kept down to no more than three to four mesh intervals. This requires one to build into the numerical scheme some monotonicity constraint, such as the TVD concept of Harten [14] or the positivity condition [8]. On the one hand, such properties enhance clean shock capturing by suppressing non-physical oscillations near flow discontinuities. On the other hand, they tend to clip spiky pressure profiles, so they are somewhat incompatible with the flow features that typify detonation waves. Although based on one-dimensional physics, their performance is frequently not degraded by much when extended to multidimensional problems. Random-choice based techniques have the unique feature that one-dimensional discontinuities in the data are preserved as sharp discontinuities at all later times. These techniques are ideal for the representation of shocks and contact surfaces but are notorious for suffering from noisiness in smooth flow regions, a feature which is further amplified by the presence of source terms in the equations. Multidimensional extensions of random-choice based techniques are not able to reproduce the clean one-dimensional performance.

(3.1) *The Detonation Analogue*

Testing the various candidate techniques on the full unsteady reactive Euler equations (5) would have been a very time consuming and expensive exercise. To speed up the process and remain within affordable costs, we have used a model test problem, namely the detonation analogue proposed by Fickett [10], as the basis for selecting the most suitable numerical scheme. The detonation analogue consists of a reduced two-by-two system of equations, but at the same time retains the essential characteristics of a physical detonation, namely strong shocks which initiate strong chemical activity. It is therefore likely to pose numerical difficulties similar to the ones encountered in a more realistic calculation. It also possesses exact steady solutions which are helpful in assessing the results. The main limitation of the detonation analogue is the absence of a left moving wave system, implying that wave phenomena involving reflections cannot be accounted for by the model. This still leaves a large class of problems for which the model is adequate. We next discuss Fickett's detonation analogue and briefly describe its likely solutions.

The model, written in conservation form with source terms, reads

$$\mathbf{W}_t + \mathbf{F}(\mathbf{W})_x = \mathbf{S}(\mathbf{W}) \tag{9a}$$

$$\mathbf{W} = (\rho, \lambda)^{\mathrm{T}}$$

$$\mathbf{F} = (p, 0)^{\mathrm{T}} \tag{9b}$$

$$\mathbf{S} = (0, r)^{\mathrm{T}}$$

with

$$p = \tfrac{1}{2}\rho^2 + \tfrac{1}{2}\lambda Q \tag{9c}$$

$$r(\lambda) = 2(1-\lambda)^{1/2}. \tag{9d}$$

Ignoring dimensional inconsistencies, the variables ρ, p, λ, and Q play similar roles as in (5). Equation (9) can be regarded as a reactive form of the inviscid Burger's equation.

In matrix form, (9) reads

$$\begin{pmatrix}\rho\\ \lambda\end{pmatrix}_t + \begin{pmatrix}\rho & \frac{1}{2}Q\\ 0 & 0\end{pmatrix}\begin{pmatrix}\rho\\ \lambda\end{pmatrix}_x = \begin{pmatrix}0\\ r\end{pmatrix}, \tag{10}$$

admitting two characteristic speeds $\lambda_1 = 0$ and $\lambda_2 = \rho$. The matrix of right eigenvectors is given by

$$R = \begin{pmatrix} 1 & 1\\ -\dfrac{2\rho}{Q} & 0\end{pmatrix}. \tag{11}$$

The model admits shocks S with jump condition

$$S = [p]/[\rho]. \tag{12}$$

By (9b), λ remains continuous across a shock; hence (12) reduces to

$$S = [\tfrac{1}{2}\rho^2]/[\rho] = \tfrac{1}{2}(\rho^- + \rho^+) \tag{13}$$

with $(\,)^{\pm}$ referring to conditions on either side of the shock.

Transforming the equations to a frame of reference attached to the shock, moving at a constant speed S, exact steady solutions, i.e., propagating waves, can be obtained which read

$$\rho = S + [S^2 - Q(2-t)t]^{1/2} \tag{14}$$

with $0 \leqslant t \leqslant 1$. The solution is valid from the leading shock ($\lambda = t = 0$) through to the tail of the reaction zone ($\lambda = t = 1$) (for details see [10, 5]). Likely solution profiles are depicted in Fig. 1, where the value ρ_b specified on the left-hand

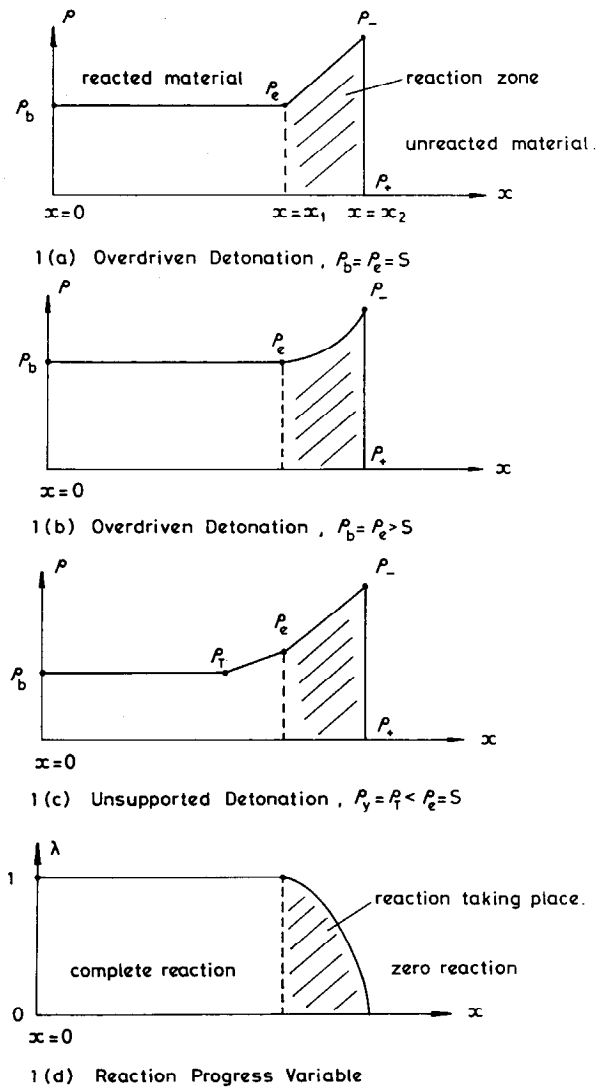

FIG. 1. Likely steady solution profiles of the detonation analogue (9).

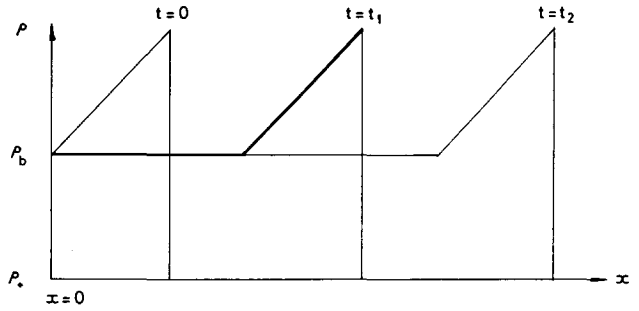

FIG. 2. Denotation analogue (9): Steady CJ propagating wave.

boundary selects one of the three possible cases, according to whether ρ_b is equal, less than, or greater than S. These cases are referred to as a CJ wave, unsupported detonation, and overdriven detonation, respectively. Figure 1d depicts a typical profile of the reaction progress variable for all three cases.

(3.2) *Test Problems*

We consider two test problems, illustrated in Figs. 2 and 3.

PROBLEM 1. The initial condition is the steady exact solution (14) with $S^2 = Q$. For this particular choice, ρ in linearly distributed across the reaction, and ρ_e at the tail of the reaction zone is equal to S, the steady shock speed. The density on the boundary is $\rho_b = \rho_e = S$. The profile should be convected without distortion by the numerical scheme. Although this is probably the simplest test one can devise for the analogue, it already serves to discard some of the numerical methods used (see Fig. 2).

PROBLEM 2. The initial condition is a uniform shock with $\rho_b = \rho_e = S$. The reaction is initiated. The combination of shock and reaction should develop into the steady profile of Problem 1, the exact form of which is known (see Fig. 3).

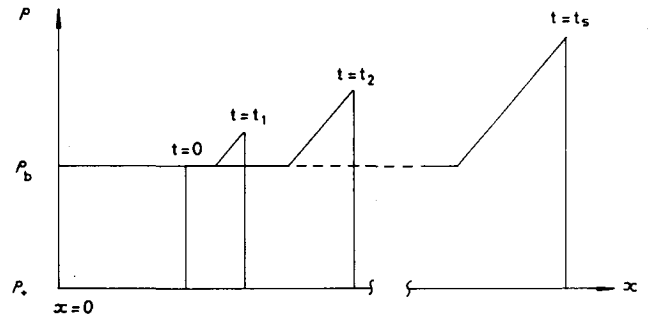

FIG. 3. Detonation analogue (9): Uniform shock developing into a steady CJ propagating wave.

The "ignition criterion" used to switch source terms on is $\rho > \rho_{act}$, with $\rho_{act} = 4.0$.

(3.3) *Numerical Schemes*

In the following, $\mathbf{W}$ denotes the vector of unknowns, $\mathbf{F}$ the vector of flux functions, and $\mathbf{S}$ the vector of source terms. Six numerical methods are considered which are briefly described below for homogeneous systems. The source terms are incorporated into the algorithm via time operator splitting, using the simple forward Euler formula for ordinary differential equations (ODEs). For more complicated rate equations, this may not be sufficient and alternative integrators may be needed (e.g., Runge–Kutta type or even stiff integrators). All our candidate methods are explicit, even though an implicit method would have allowed us to incorporate stiff source terms within the scheme without resorting to splitting. However, it is well known that implicit schemes do not show any advantage (and are usually decidedly disadvantageous) for transient shock problems without reaction. A second procedure is to treat only the reaction equations implicitly, as in Yee and Shinn [31], but his did not prove necessary for out simple model problem.

The MacCormack Method. This is a two-step prediction–correction variant of the Lax–Wendroff finite difference scheme [18],

$$\mathbf{W}_j^* = \mathbf{W}_j^n - \frac{\Delta T}{\Delta X}[\mathbf{F}(\mathbf{W}_{j+1}^n) - \mathbf{F}(\mathbf{W}_j^n)]$$

$$\mathbf{W}_j^{n+1} = \frac{1}{2}(\mathbf{W}_j^* + \mathbf{W}_j^n) - \frac{\Delta T}{2\Delta x}\left[\mathbf{F}(\mathbf{W}_j^*) - \mathbf{F}(\mathbf{W}_{j-1}^*)\right].$$

Practical applications normally involve the use of artificial viscosity to enhance stability, which will not be discussed here (see [18, 1]).

Godunov's Method. This two-step method [13] uses the solution of the Riemann problem to obtain provisional values for intercell fluxes. It takes the form

$$\mathbf{W}_j^{n+1} = \mathbf{W}_j^n - \frac{\Delta T}{\Delta X}[\mathbf{F}(\mathbf{W}_{j+1/2}^{n+1/2}) - \mathbf{F}(\mathbf{W}_{j-1/2}^{n+1/2})],$$

where $\mathbf{W}_{j\pm 1/2}^{n+1/2}$ are the solution of the Riemann problem with data $\mathbf{W}_j^n$ and $\mathbf{W}_{j\pm 1}^n$ at the respective cell interfaces. Details of the exact solution to the Riemann problem for the homogeneous detonation analogue (i.e., (10) without the source terms) can be found in [5].

The Random Choice Method (RCM). The RCM, originally proposed by Chorin [4], is again a Riemann problem-based technique. It solves the two Riemann problems at cell interfaces $j \pm 1/2$ and assigns $\mathbf{W}_j^{n+1}$ a value

based on a random sampling of the exact solution inside the cell j at time level $n+1$. The random sampling uses the van der Corput sequence of pseudo random numbers [6]. The method possesses the unique feature that it is able to represent discontinuities with zero width but has a random error in their position.

Higher Order RCM. The higher order RCM, is essentially a random generalisation of Godunov's scheme, namely

$$\mathbf{W}_j^{n+1} = \mathbf{W}_j^n - \frac{\Delta T}{\Delta X}[\mathbf{F}(\xi; j, j+1) - \mathbf{F}(\xi; j, j-1)],$$

where $\mathbf{F}(\xi; j, j+1)$ is based on exact solution of the Riemann problem and is evaluated at a random position ξ in the interval $(j, j+1)$, at half time level. A hybridised version of this method is also studied, where the traditional RCM is used at large discontinuities (see [29]).

Flux Difference Splitting Method (Roe's Scheme). This method [22] uses an approximate Riemann solver to model wave interaction at cell interfaces. It uses the exact solution of a locally linearised model

$$\mathbf{W}_t + \tilde{A}(\mathbf{W}_L, \mathbf{W}_R)\,\mathbf{W}_x = 0,$$

where $\tilde{A}$ is a local average of the Jacobian matrix in (10), satisfying

$$\tilde{A}(\mathbf{W}_L, \mathbf{W}_R)(\mathbf{W}_R - \mathbf{W}_L) = (\mathbf{F}_R - \mathbf{F}_L). \tag{15}$$

This property ensures that the solution to the linearised problem is exact if the data correspond to a single discontinuity. For the detonation analogue, the average $\tilde{A}$ is as in (10), with ρ replaced by $\tilde{\rho} = \frac{1}{2}(\rho_L + \rho_R)$. The method is of Godunov type with the interface flux given by

$$\mathbf{F}_{j+1/2} = \tfrac{1}{2}(\mathbf{F}_L + \mathbf{F}_R) - \tfrac{1}{2}\sum_k \alpha_k |\tilde{\lambda}_k| [1 - \varphi_k(1 - |\tilde{\nu}_k|)]\,\tilde{\mathbf{r}}_k. \tag{16}$$

Here, $\tilde{\lambda}_k$ and $\tilde{\mathbf{r}}_k$ are the eigenvalues and right eigenvectors of $\tilde{A}$, α_k are the local wave strengths, $\tilde{\nu}_k = \tilde{\lambda}_k \Delta T/\Delta X$ are the local CFL numbers, and φ_k is a limiter function equal to zero in non-smooth flow regions but close to one in smooth regions. We used the superbee flux limiter [28].

Moving Finite Element Method (MFE). Like the standard finite element method, the MFE method is based on projecting the solution into an approximation normed space and minimising the error of the solution by an optimal choice of coefficients. It has the additional feature that it allows grid nodes to move to areas of large gradients, their motion being determined by the same minimisation algorithm. The original MFE was first introduced by Miller and Miller [19] and has been successfully applied to homogeneous hyperbolic problems. The algorithm begins by expanding $\mathbf{W}$ in a set of linear basis functions α_j with nodal amplitudes a_j,

$$\mathbf{W} = \sum_j a_j \alpha_j.$$

The basis functions $\alpha_j = \alpha_j(\mathbf{X}, \mathbf{S})$, are linear functions of compact support, and $\mathbf{S} = \mathbf{S}(t)$ is a time-dependent vector of nodal positions S_j. Differentiating $\mathbf{W}$ with respect to time and projecting the flux $\mathbf{F}$ into the same space leads to an L_2 minimisation problem of the residual

$$\|\mathbf{W}_t + \mathbf{F}(\mathbf{W})_x\|_2$$

over the parameters $\dot{a}_j(t)$ and $\dot{S}_j(t)$. Amplitude and nodal

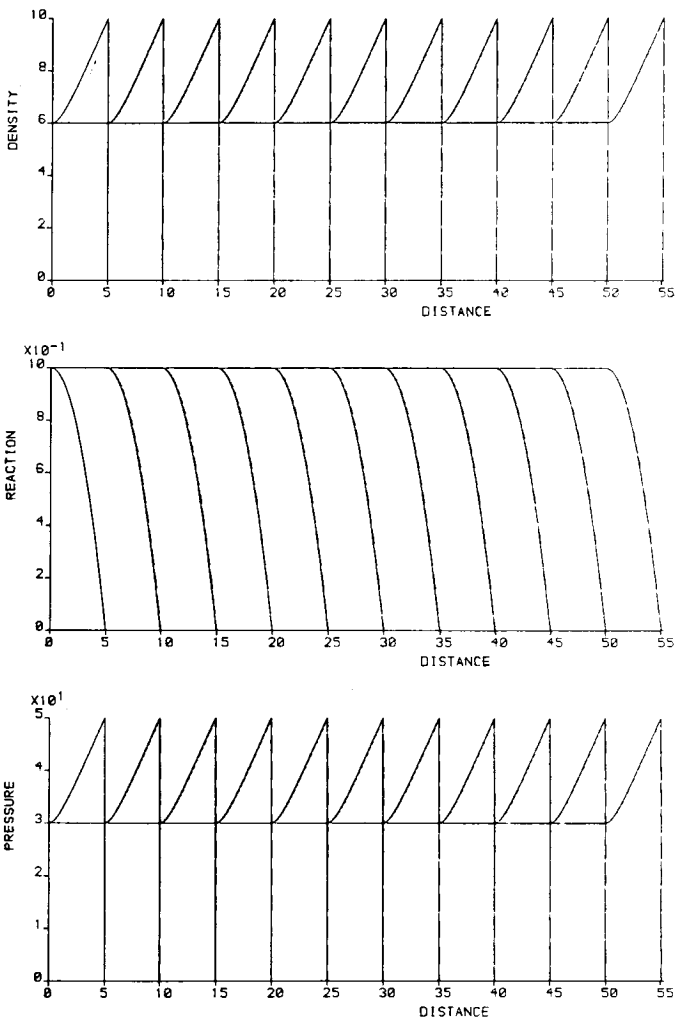

FIG. 4. Detonation analogue (9): Steady CJ wave by MFE method, MEM-computed (dotted) and exact (full) solutions.

motion are then determined by solving a set of ODEs. The nodal paths $X = S_j(t)$ are found to be approximations to the characteristic curves of the system, so that nodal values $a_j(t)$ are almost independent of time. Our method followed the general lines of the version referred to by Edwards [7] as the mobile element method. We comment further on this method in the next section.

(3.4) *Assessment of Methods*

All the results, with the exception of the MFE, are for a fixed regular mesh. The mesh size $DX = 0.5$ is such that the reaction zone is discretised by 10 points, which seemed a reasonable resolution to aim for in realistic problems. Figures are shown for selected schemes only.

Results for Problem 1. The MFE method (Fig. 4) produces perfect results. This should not come as a surprise since, by construction, all nodes are moving at the shock speed S and the steady problem is somewhat redundant.

The RCM (Fig. 5) preserves a sharp shock profile although its position is affected by randomness. Peak shock values are very accurate. The discontinuity in density-derivative at the tail of the reaction zone is also accurately captured. The reaction zone has the correct width but the flow profile inside it is also affected by randomness. The randomness in the reaction zone can be eliminated by using the hybrid version of higher order RCM, although it is still apparent in the shock position where standard RCM is used.

Godunov's method produces smeared shocks and rounds the tail of the reaction zone. Consequently, the reaction zone appears to occupy twice the correct width after about 10 time units. Also, frozen shock values are not attained accurately.

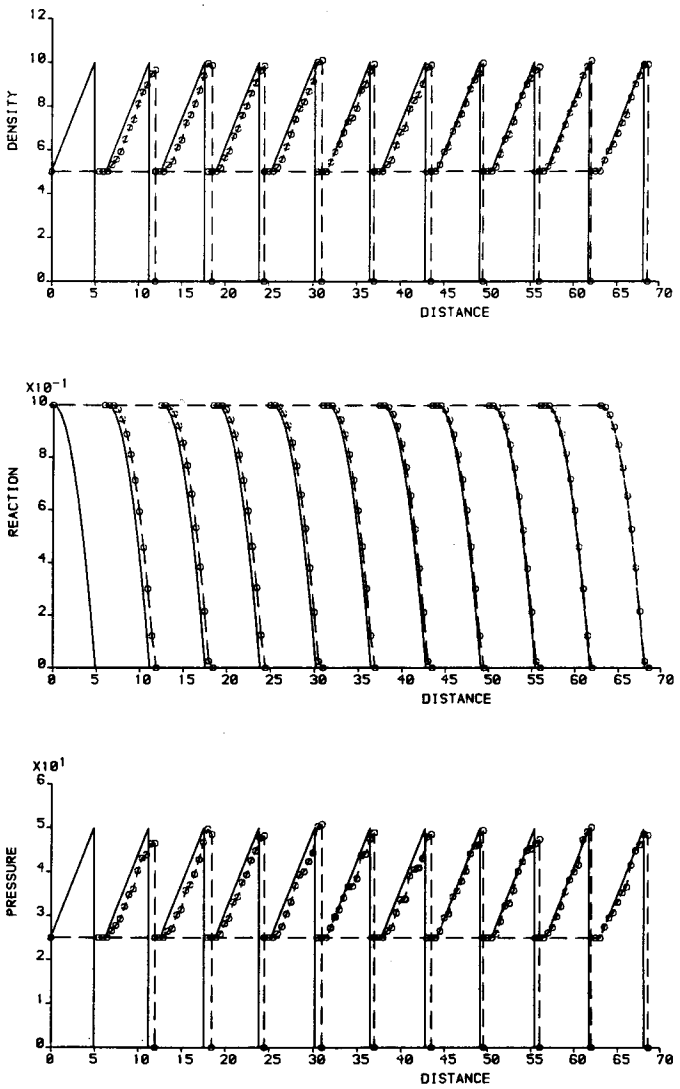

FIG. 5. Detonation analogue (9): Steady CJ wave by RCM method and exact solution (full line).

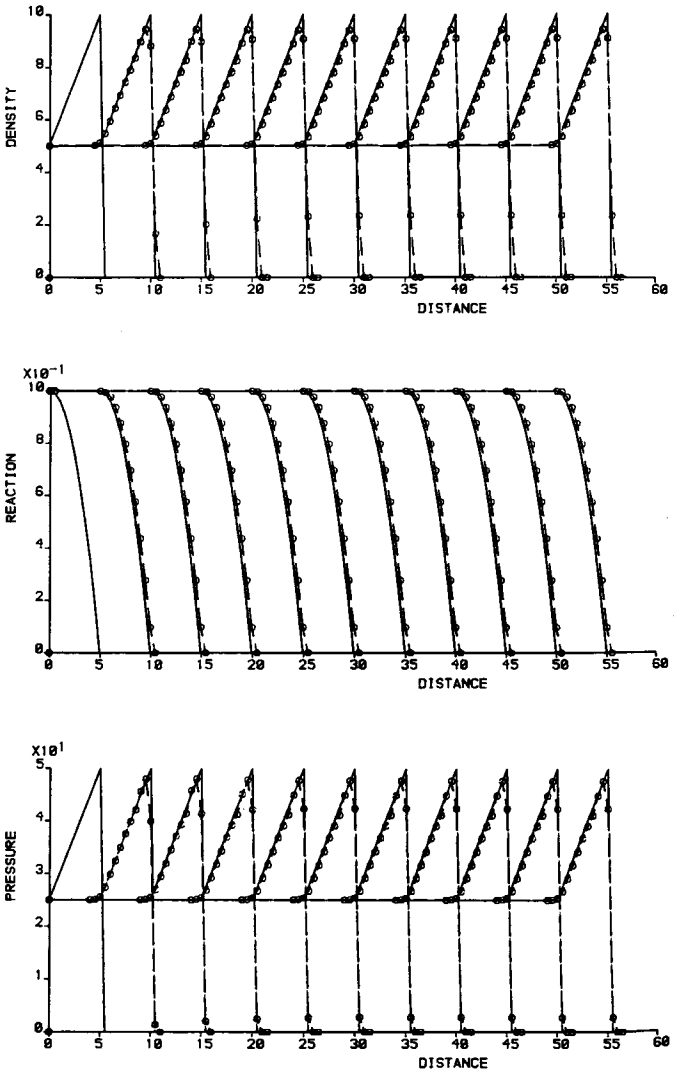

FIG. 6. Detonation analogue (9): Steady CJ wave by Roe's method and exact solution (full).

Roe's method produces very satisfactory results (Fig. 6). The shock profile is reasonably sharp and shock peak values are reasonably accurate.

Finally, the MacCormack scheme produces typical density oscillation behind the shock which completely contaminates the reaction zone. The density-based ignition criterion causes the reaction to stop temporarily due to density undershoots. This affects the λ profiles which should otherwise be smooth, since the rate equation itself is independent of ρ. For more realistic rate equations, λ profiles are expected to be worse. The method as applied (no artificial viscosity) is clearly inadequate.

Results for Problem 2. On the basis of the previous results, we have excluded the MacCormack and Godunov's schemes. We have also excluded the MFE method. We did not succeed in producing acceptable results for this more realistic unsteady problem. As nodes follow characteristic paths, they are removed from the reaction zone without being replaced, leading to poor resolution of flow features (Fig. 7). We do not rule out the possibility that some way of rescuing the MFE method can be found, but we expect that it will not be easy. The performance of the rest of the methods is similar to Problem 1. They all proved capable of initiating the detonation and carrying it to a steady state in about the same time (See Figs. 8 and 9).

Conclusions. We found MacCormack, Godunov, and MFE inadequate for the modelling of unsteady detonations. The remaining methods, RCM, Hybrid, and Roe, all produced satisfactory results. In view of the fundamental difficulty in extending random choice based techniques to more than one space dimension, and in view of the growing experience in applying Roe's method to multidimensional

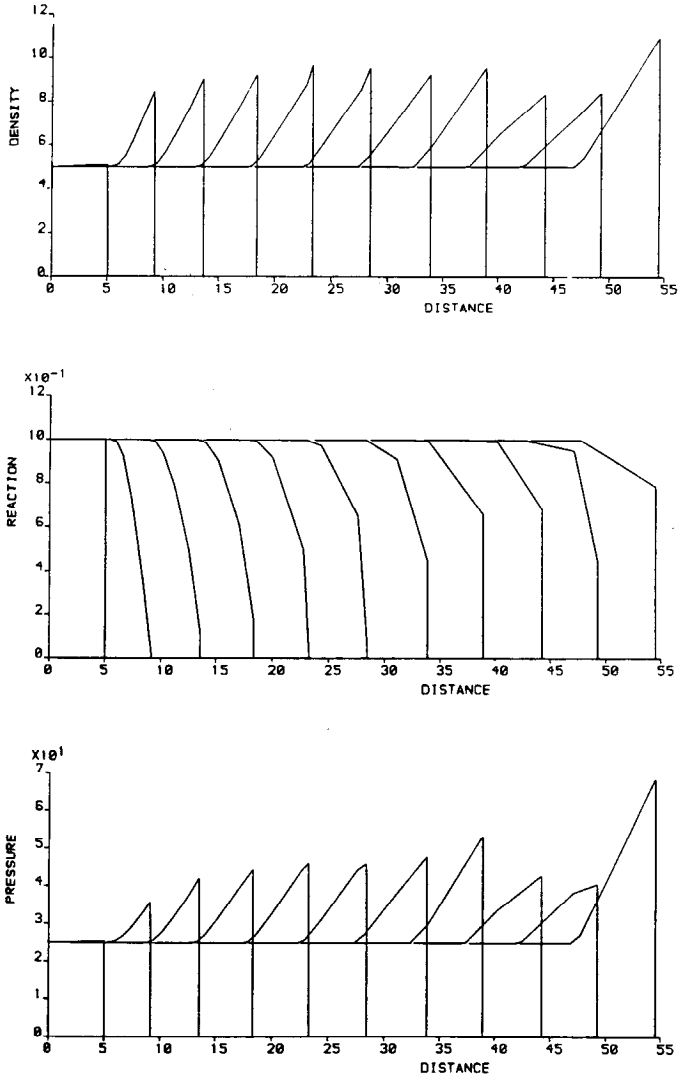

FIG. 7. Detonation analogue (9): Unsteady CJ wave by MFE method, computed (dotted) and exact (full) solutions.

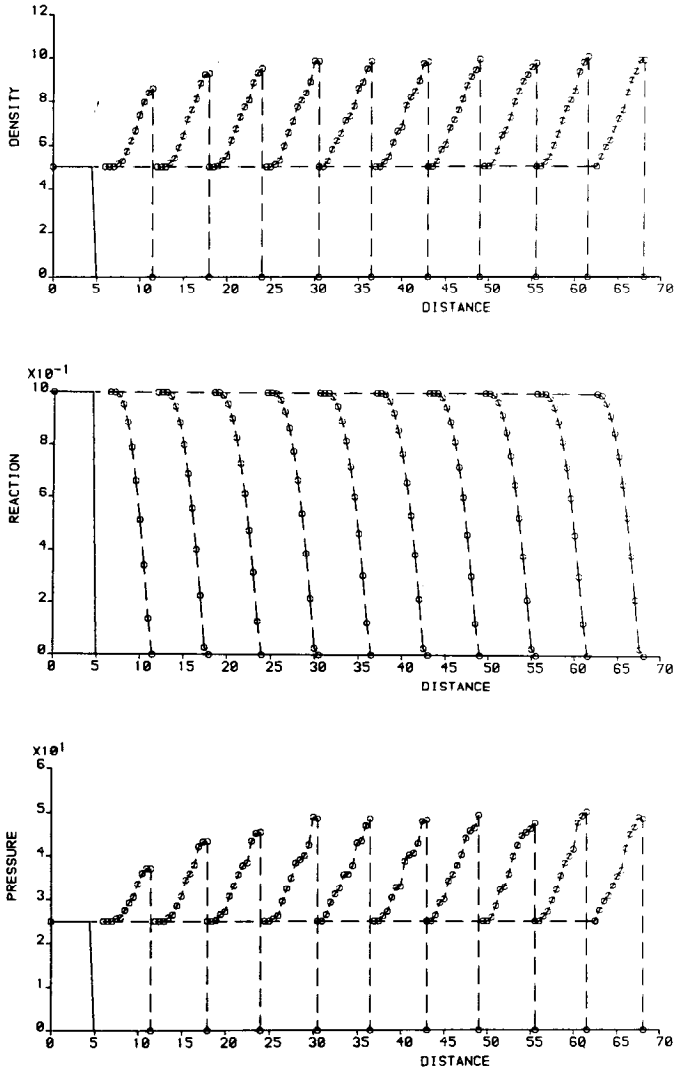

FIG. 8. Detonation analogue (9): Unsteady CJ wave by RCM method.

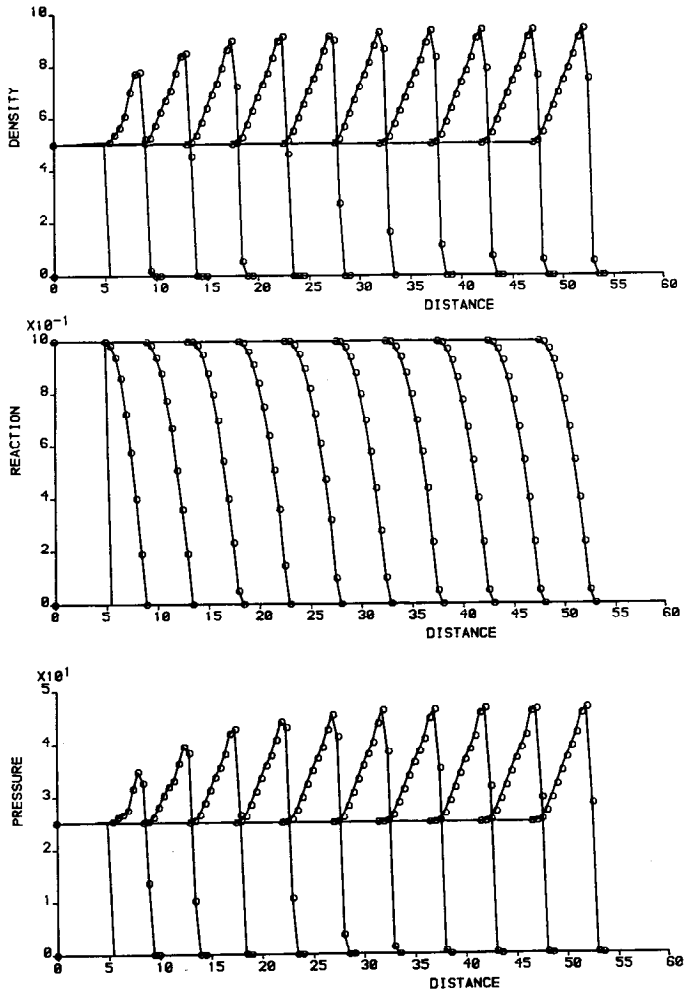

FIG. 9. Detonation analogue (9): Unsteady CJ wave by Roe's method.

problems with complicated equations of states, using irregular and adaptive grids, we have selected Roe's method to solve the 2D unsteady reactive Euler equations (5).

4. EXTENSION OF ROE'S METHOD

The system we wish to solve can be written in matrix form,

$$\mathbf{W}_t + A(\mathbf{W})\,\mathbf{W}_x + B(\mathbf{W})\,\mathbf{W}_y = \mathbf{S}(\mathbf{W}) \tag{17}$$

with $A(\mathbf{W}) = \partial\mathbf{F}/\partial\mathbf{W}$ and $B(\mathbf{W}) = \partial\mathbf{G}/\partial\mathbf{W}$ given by (6). The algorithm we use is a space-time operator split algorithm, where the solution is evolved in three decoupled stages,

$$\begin{aligned} \mathbf{W}_t + A(\mathbf{W})\,\mathbf{W}_x &= 0 \\ \mathbf{W}_t + B(\mathbf{W})\,\mathbf{W}_y &= 0 \\ \mathbf{W}_t &= \mathbf{S}(\mathbf{W}). \end{aligned} \tag{18}$$

Each of the first two stages (18a), (18b) is solved using an extended solver of Roe type. The third stage (18c) requires an ODE time integrator.

We now describe the one-dimensional Roe solver in the x direction. The solver in the y direction follows in an analogous fashion. The approximate Riemann solver used by Roe's method is based on local linearisation of the Jacobian matrices. For consistent shock capturing [22], the Jacobian matrix A is to be evaluated at some data-dependent average state $\tilde{A} = \tilde{A}(\tilde{\mathbf{W}})$, $\tilde{\mathbf{W}} = \tilde{\mathbf{W}}(\mathbf{W}_L, \mathbf{W}_R)$ such that the Roe condition (15) is satisfied, for two arbitrary states $\mathbf{W}_L$ and $\mathbf{W}_R$. The condition (15) is an over-specified problem for which a solution may not exist. It can be shown, however, that for the present model (5) a unique linearisation does exist, which satisfies (15) with local averages,

$$\begin{aligned} \tilde{\rho} &= R\rho_{\mathrm{L}}; \qquad R = \sqrt{\rho_{\mathrm{R}}/\rho_{\mathrm{L}}} \\ \tilde{u} &= (u_{\mathrm{L}} + Ru_{\mathrm{R}})/(1+R) \\ \tilde{v} &= (v_{\mathrm{L}} + Rv_{\mathrm{R}})/(1+R) \\ \tilde{H} &= (H_{\mathrm{L}} + RH_{\mathrm{R}})/(1+R) \\ \tilde{\lambda} &= (\lambda_{\mathrm{L}} + R\lambda_{\mathrm{R}})/(1+R) \\ \tilde{Q} &= (Q_{\mathrm{L}} + RQ_{\mathrm{R}})/(1+R) \end{aligned} \tag{19}$$

and the average speed of sound is calculated from

$$\tilde{a}^2 = (\gamma - 1)[\tilde{H} - \tfrac{1}{2}(\tilde{u}^2 + \tilde{v}^2) + \tilde{\lambda}\tilde{Q}].$$

Simple waves of the linearised problem are then identified by projecting local gradients into the characteristic fields of the system. Local wave strengths α_k are found by solving

$$\mathbf{W}_{\mathrm{R}} - \mathbf{W}_{\mathrm{L}} = \sum_k \alpha_k \tilde{\mathbf{r}}_k,$$

where $\tilde{\mathbf{r}}_k$ are the eigenvectors in (8), evaluated at the average state $\tilde{\mathbf{W}}$. Using $\Delta(\,) = (\,)_{\mathrm{R}} - (\,)_{\mathrm{L}}$ to denote spatial gradients, the α_k's are

$$\begin{aligned} \alpha_1 &= [\Delta p - \tilde{\rho}\tilde{a}\,\Delta u]/2\tilde{a}^2 \\ \alpha_2 &= [\tilde{a}^2\,\Delta\rho - \Delta p]/\tilde{a}^2 \\ \alpha_3 &= \tilde{\rho}\,\Delta v \\ \alpha_4 &= \tilde{\rho}\,\Delta\lambda + \tfrac{1}{2}\tilde{\lambda}\alpha_2 \\ \alpha_5 &= \tilde{\rho}\,\Delta Q + \tfrac{1}{2}\tilde{Q}\alpha_2 \\ \alpha_6 &= [\Delta p + \tilde{\rho}\tilde{a}\,\Delta u]/2\tilde{a}^2. \end{aligned} \tag{20}$$

The solution is then updated by a Godunov-type formula,

$$\mathbf{W}^*_{i,j} = \mathbf{W}^n_{i,j} - \frac{\Delta T}{\Delta X}[\mathbf{F}^n_{i,j+1/2} - \mathbf{F}^n_{i,j-1/2}].$$

The intercell fluxes are given by

$$\mathbf{F}_{i,j+1/2} = \tfrac{1}{2}(\mathbf{F}_L + \mathbf{F}_R) - \tfrac{1}{2}\sum_k \alpha_k |\tilde{\lambda}_k| [1 - \varphi_k(1 - |\tilde{\nu}_k|)] \tilde{\mathbf{r}}_k.$$

Having obtained predicted $\mathbf{W}^*$ values via flux updates in the main directions, a corrected value is calculated which accounts for the source contribution. For the simple rate equation used by the model (5), it has proved sufficient to apply a forward Euler integrator

$$\mathbf{W}_{i,j}^{n+1} = \mathbf{W}_{i,j}^* + \Delta T \cdot \mathbf{S}(\mathbf{W}_{i,j}^*). \tag{21}$$

Stable and accurate time integration of more complicated rate equations will probably require more elaborate integrators, e.g., Runge–Kutta type integrators. Since time scales associated with the chemical reaction are typically several orders of magnitude smaller than those associated than for the rest of the governing equations, and the small prospective gains in accuracy are outweighed by the added computational inconvenience. A crude cure that has been considered is to force $Q_{i,j}$ to lie inside the range $[Q_{\min}, Q_{\max}]$, but was found unstable. We have also considered a more subtle cure, based on replacing the conservative solution algorithm by a consistent primitive algorithm near the interface [15]. The primitive algorithm, suitably modified to account for leading conservation errors, has offered accuracy gains near contact surfaces in other two-phase flow models which did not include chemical reactions [16]. In the present model, however, applying the primitive algorithm only in certain flow regions led to instabilities.

Since nodal values of Q are only used in the ignition criterion (22), these small overshoots in Q profiles are not believed to present a serious computational difficulty, but rather an aesthetic one. The tactic which has proved best is to let Q profiles settle without taking any external measures. Indeed, the early overshoots in Q gradually disappear (see Fig. 10).

integrators [17].

An "ignition criterion" is used, based on predicted pressure and heat release variable estimates,

$$\begin{array}{ll} p_{i,j} > p_{\text{act}}; \quad Q_{i,j} > Q_{\text{act}} & \text{sources activated} \\ \text{otherwise} & \text{sources not activated.} \end{array} \tag{22}$$

There are still several unresolved problems with the model and the proposed algorithm:

Oscillations in Q. The sixth component of Eq. (5) is incorporated into the model in order to allow the distinction between materials with different heat release constants and, in particular, between reacting and non-reacting flow regions. Local values of the heat release variable are calculated from a conservative update of ρ and ρQ,

$$Q_{i,j}^{n+1} = \frac{(\rho Q)_{i,j}^{n+1}}{(\rho)_{i,j}^{n+1}} \tag{23}$$

and are expected to approximate a piecewise constant function, separated by contours of material discontinuities. Across the non-uniform regions, $Q_{i,j}$ is expected to change monotonically from $Q_{\min}$ to $Q_{\max}$ with the value $0.5(Q_{\min} + Q_{\max})$ marking the material interface. Although both (ρQ) and (ρ) change monotonically across contact surfaces, Q worked out from (23) need not necessarily do so. Indeed, small overshoots in Q profiles can be observed, mainly in very early stages of the calculations.

One possible remedy is to use the primitive form (4), so that Q itself is one of the flow variables solved for. Numerically, this will require a different solution algorithm for Q

Negative internal energies. This phenomenon is not unique to reactive flow modelling. It may also occur in non-reactive models, but it tends to be amplified by the chemical

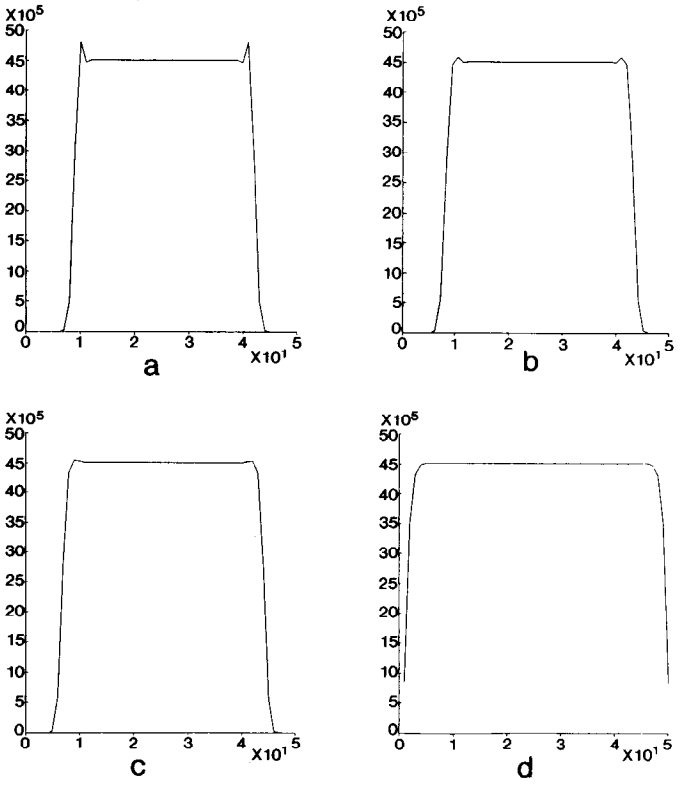

FIG. 10. Two-dimensional reactive Euler equations (5): oscillation in Q near material interfaces: Computed solution after (a) 10, (b) 20, (c) 30, and (d) 70 time steps.

activity. It has been observed that under certain flow conditions, particularly near low densities, the code may predict negative pressures/densities. This immediately leads to a failure of the scheme through the calculation of the local sound speed. Crude replacement of negative values by positive ones not only destroys conservation, but was also found to be unstable. As analysed in [9] for non-reactive flow models, this failure may occur with any Godunov-type scheme based on a linearized Riemann solver. For the particular case of Roe's scheme, the "explanation" for the failure was that the numerical signal velocities predicted by the local linearization underestimated the physical signal velocities. A condition has been established to ensure that densities and internal energies remain positive by suitably modifying the numerical signal-speeds in the dangerous regions. As it is, this condition is applicable only to non-reactive flows and the analysis is strictly valid for the first-order version of Roe's scheme and for certain simplified data. Similar analysis is required for the reactive case, which is further complicated by the presence of source terms. To data, this has not been done.

5. ADAPTIVE GRIDDING

It is easily demonstrated that some form of adaptive gridding is a pre-requisite for the computation of detonation driven flows produced by explosive devices such as the rate-stick. For example, consider a cylindrical charge of Hmx-based explosive with diameter 80 mm and length 100 mm. The reaction zone for this type of explosive can be as narrow as 0.022 mm. Now, calculations to model problems indicate that at least 10 mesh cells are required to adequately resolve the reaction zone. Consequently, if a uniform mesh is used to discretize the computational domain then an axi-symmetric calculation would require some 8×10^6 mesh cells, while a full three-dimensional calculation would need 4×10^{10} mesh cells. These grids would be much too large for practical purposes. However, an adaptive gridding technique could significantly reduce, possibly by several orders of magnitude, the number of cells required to discretize the computational domain.

Many different adaptive grid strategies have been described in the literature, but space does not permit a discussion of the relative merits of these schemes applied to detonation problems. Suffice it to say that we have chosen a method that is loosely based on that proposed by Berger [2]. Here, we simply attempt to impart the main features of the scheme and note that full details are given by Quirk in [21].

The computational domain is discretized into a set of embedded meshes. Each mesh forms a logically rectangular patch ruled by I, J co-ordinate lines, and these lines are continuous between neighbouring patches. An embedded patch refines part of an underlying coarse patch. The cells of the embedded patch are formed by sub-dividing coarse patch cells. The number of sub-divisions along the I and J co-ordinate lines are arbitrary integers and are typically set to four. It is possible to group the meshes to form a hierarchical grid system. A level l is associated with each mesh, this represents the number of coarser meshes underlying a given mesh. Thus, the coarsest mesh is at level 0, and progressively finer meshes are at levels 1, 2, ..., $l_{\max}$. The meshes at level l may be grouped together to form the effective grid at level l, namely G_l. Fine meshes at level l must be embedded in coarser meshes at level $l-1$, therefore it follows that the fine grid G_l is wholly embedded in the coarse grid G_{l-1}, $G_l \subseteq G_{l-1}$. Figure (11a) shows a fine grid, G_2, embedded in a medium grid G_1, which in turn is embedded in a coarse grid G_0. It is important to note that there is a continuous coarse grid, and a coarse grid solution below every embedded mesh, see Fig. (11b).

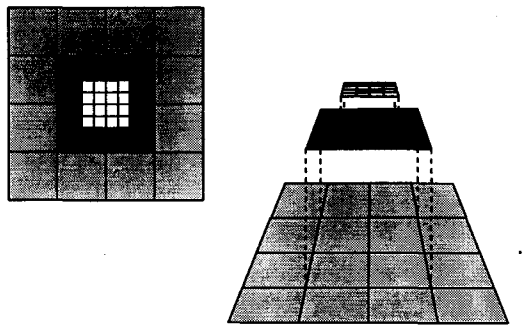

FIG. 11. Three grid levels: Coarse, medium, and fine.

The scheme also refines in time as well as in space; also, smaller time steps are taken on fine grids than on coarse grids. This refinement in time makes the adaptive procedure particularly suitable for detonation calculations. It allows comparable Courant numbers to be used during the integration process of each grid level. This improves the accuracy of the integration process, since a Lax–Wendroff

TABLE I

Order of Grid Integration

Grid integrated	Time step
$G0$	$\Delta t0$
$G1$	$\Delta t0/2$
$G2$	$\Delta t0/4$
$G2$	$\Delta t0/4$
$G1$	$\Delta t0/2$
$G2$	$\Delta t0/4$
$G2$	$\Delta t0/4$

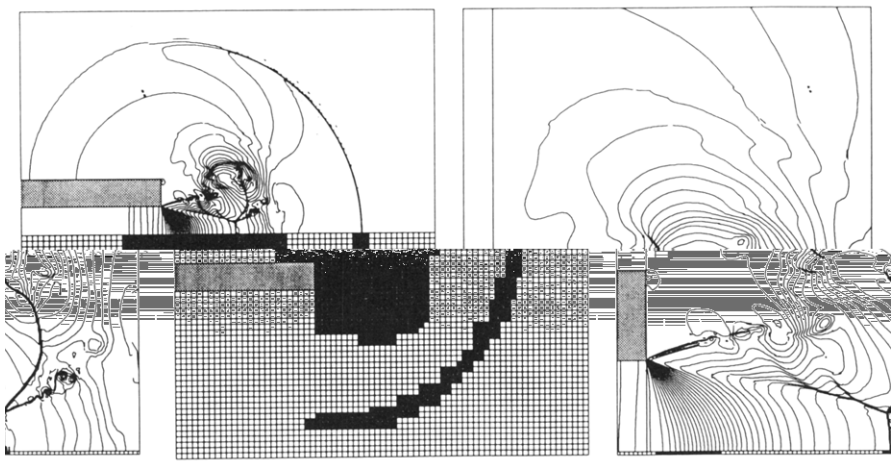

FIG. 12. Adaptive grid calculation: Plane shock escaping from an open-ended shock tube.

scheme is most accurate for Courant numbers of one. If the same time step was used for every cell in the computational domain then cells away from the reaction zone would be integrated with extremely small Courant numbers. This could have an adverse effect on the accuracy of the calculation and would also be computationally wasteful. Because more integrations are done on fine grids than on coarse grids, the order of grid integration must be carefully coordinated. This order for the grid structure shown in Table I. Note the recursive interleaving of the different grid levels. During the integration process, coarse grids effectively provide boundary conditions for the embedded fine grids. This process requires the interpolation in time of the coarse grid solution at the embedded fine mesh boundary. Interleaving the order of grid integration minimizes the time span over which it is necessary to interpolate.

The adaption of the grid structure to an evolving flow results in the embedded grids gliding along their respective underlying coarse grids so as to keep pace with any discontinuities within the flow field. This process is completely automatic and has proved very robust for computing solutions to the unreactive Euler equations. Figure 12 shows the density contours that are computed for a plane shock escaping from an open-ended shock tube. The flow is assumed to be axi-symmetric and so we need only to compute a solution for the top half of the tube. A coarse mesh of 70 by 40 cells was used to discretize the computational domain. Two levels of embedded grids were employed, each having a spatial refinement factor of four. Thus the finest level grid has the same resolution as a uniform grid of 1200 by 640 cells. The quality and accuracy of these results may be gauged by comparing them with those calculated by Wang and Widhopf [30]. The calculation was performed on a Sun sparcstation I and took less than 12 h of CPU time. An analysis of the program using UNIX profiling command *gprof* indicates that only 0.8% of the processing time was spent on the grid adaptation. It was not possible to perform this calculation on the equivalent uniform mesh, so it is not possible to give an exact figure for the relative processing time required for the adaptive and non-adaptive calculations. However, estimates based on calculations made with coarser grids suggest that the non-adaptive calculation could require as much as 30 times the processing time required by the adaptive calculation.

6. NUMERICAL TESTS

We consider two test problems:

Problem 1. Initial conditions correspond to the steady exact solution of a one-dimensional CJ wave. The reaction zone is discretised by 10 grid nodes and the detonation profile should be convected without distortion by the scheme. Data for an exact solution are given in [11] on an irregular grid. The data is transformed onto a regular grid using linear interpolation. The interpolated values are given in Table II and serve to assess the results.

TABLE II

Steady CJ Solution

t (μs)	x (mm)	p (Gpa)	u (m/s)	ρ (kg/m^3)	c (m/s)	λ
0.0	0.000	57.80	4250.0	3200.0	7361.0	0.000
0.1	0.436	54.91	4038.0	3048.0	7352.0	0.190
0.2	0.893	52.02	3825.0	2909.0	7324.0	0.360
0.3	1.371	49.13	3613.0	2783.0	7278.0	0.510
0.4	1.870	46.24	3400.0	2667.0	7212.0	0.640
0.5	2.391	43.35	3188.0	2560.0	7127.0	0.750
0.6	2.933	40.46	2975.0	2462.0	7022.0	0.840
0.7	3.496	37.57	2763.0	2370.0	6896.0	0.910
0.8	4.080	34.68	2550.0	2286.0	6747.0	0.960
0.9	1.686	31.79	2338.0	2207.0	6574.0	0.990
1.0	5.313	28.90	2125.0	2133.0	6375.0	1.000

Problem 2. This is an unsteady two-dimensional rate-stick problem, modelling a reactant encased within an inert

$$p1 = 1.0 \times 10^5 \text{ Pa}$$
$$\rho 1 = 1600.0 \text{ kg/m}^3$$
$$u1 = 0.0 \text{ m/s}$$
$$v1 = 0.0 \text{ m/s}$$
$$\lambda 1 = 0.0$$
$$Q1 = 4515600.0 \text{ J/kg}$$

$$p2 = 28.9 \times 10^9 \text{ Pa}$$
$$\rho 2 = 2133.0 \text{ kg/m}^3$$
$$u2 = 2125.0 \text{ m/s}$$
$$v2 = 0.0 \text{ m/s}$$
$$\lambda 2 = 1.0$$
$$Q2 = 4515600.0 \text{ J/kg}$$

$$p3 = 1.0 \times 10^5 \text{ Pa}$$
$$\rho 3 = 2000.0 \text{ kg/m}^3$$
$$u3 = 0.0 \text{ m/s}$$
$$v3 = 0.0 \text{ m/s}$$
$$\lambda 3 = 0.0$$
$$Q3 = 0.0 \text{ J/kg}$$

corresponding to unreacted material $(\,)_1$ (pure A), fully reacted material $(\,)_2$ (pure B) and inert high-density casing $(\,)_3$. States $(\,)_1$ and $(\,)_2$ correspond to conditions at the front and tail of the steady CJ wave of Problem 1. They are expected to initiate a reaction which, ignoring the effect of the inert casing, should develop into the detonation profile of Problem 1. The adaptive grid uses a coarse mesh of dimensions 80×32, with overlayed fine patches of refinement ratio of four covering the initial discontinuities. The problem is dependent inherently on a length scale. The calculation is performed with $DX = 0.5903$ mm, allowing the fully developed reaction zone to be represented by ten

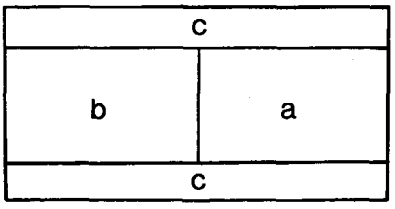

FIG. 13. Rate-stick problem initial data: (a) Unreacted material; (b) reacted material, and (c) inert casing.

Results for Problem 1. Figure 14 shows results for the steady CJ wave problem, obtained with the extended Roe's method described in Section 4. The results in general are quite good. Shock position and speed are accurate and the reaction zone is well represented. A dip in the density.profile originates inside the reaction zone, just behind the leading shock which gradually moves downstream to the tail of the detonation. It is believed to be a result of starting-up errors of the method. Similar observations were made with other methods (e.g., Godunov's method). Such start-up errors are almost inevitable features of high-resolution shock-capturing methods, if the shock profile of the initial data differs from what the algorithm accepts as a travelling-wave solution, and are commonly observed in inert-flow calculations. Here they seem more prominent, probably because the reaction spike is harder to resolve than an inert shock.

Results for Problem 2. Figures 15–23 depict density contours and adaptive grid structure for the rate-stick

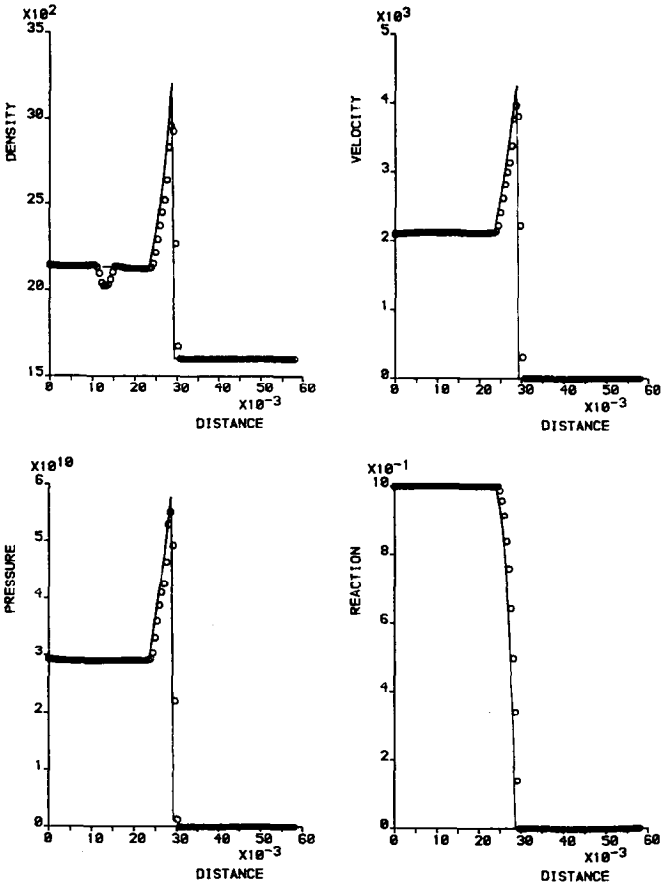

FIG. 14. One-dimensional reactive Euler equations (5): Steady CJ wave by Roe's method, exact (solid) and computed (dashed) solutions.

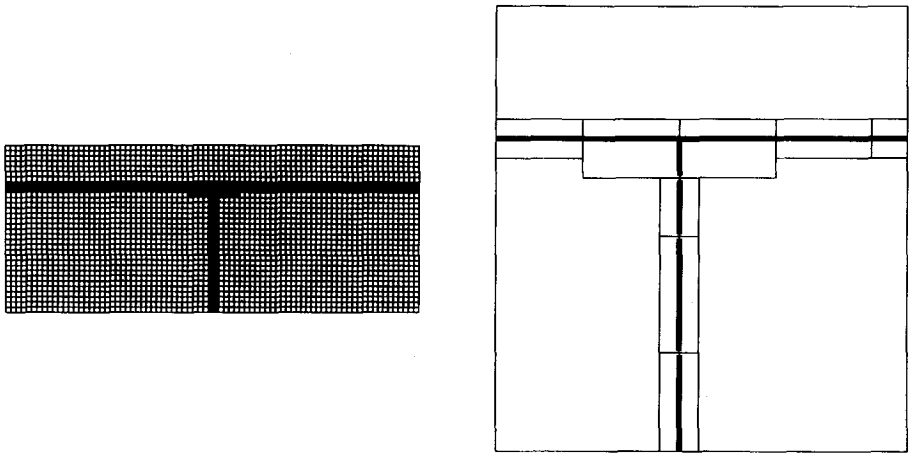

FIG. 15. Two-dimensional reactive Euler equations (5): Rate-stick problem by Roe's method, initial conditions.

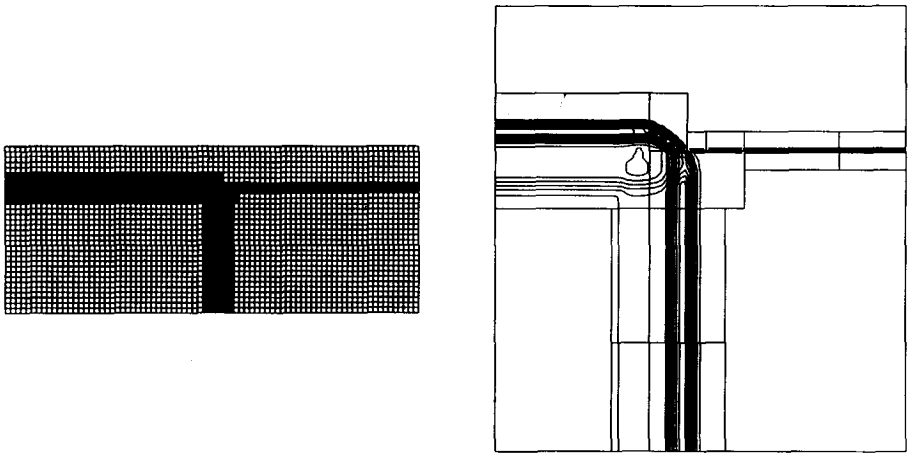

FIG. 16. Two-dimensional reactive Euler equations (5): Rate-stick problem by Roe's method, solution after 20 time steps.

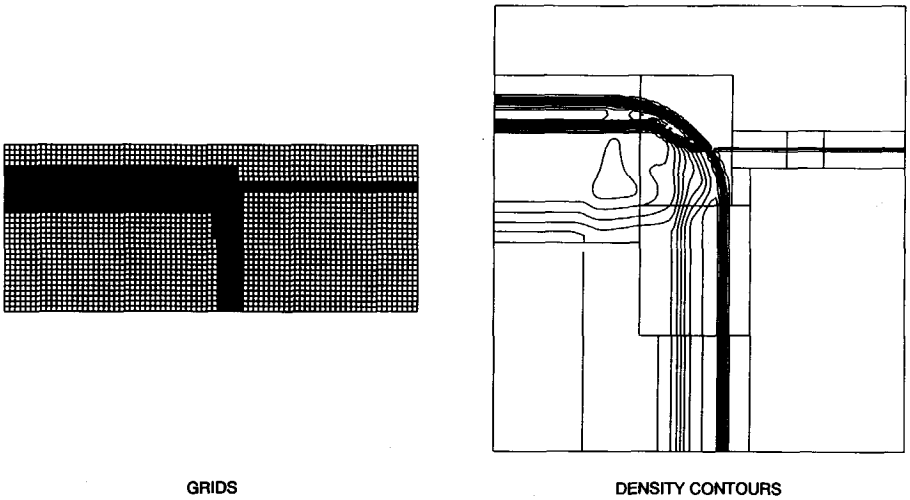

FIG. 17. Two-dimensional reactive Euler equations (5): Rate-stick problem by Roe's method, solution after 40 time steps.

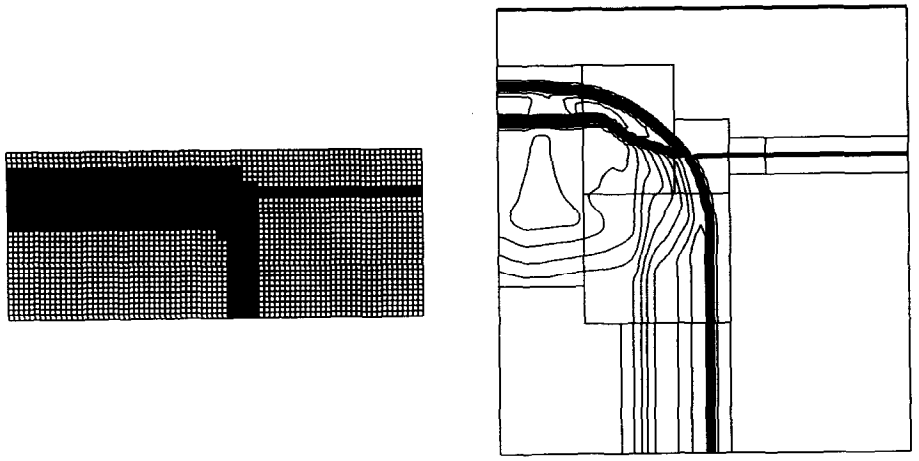

FIG. 18. Two-dimensional reactive Euler equations (5): Rate-stick problem by Roe's method, solution after 60 time steps.

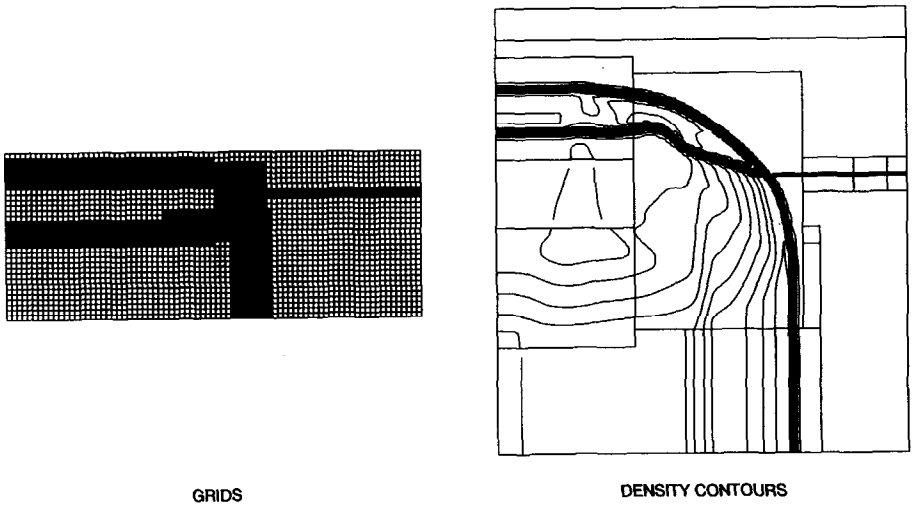

FIG. 19. Two-dimensional reactive Euler equations (5): Rate-stick problem by Roe's method, solution after 80 time steps.

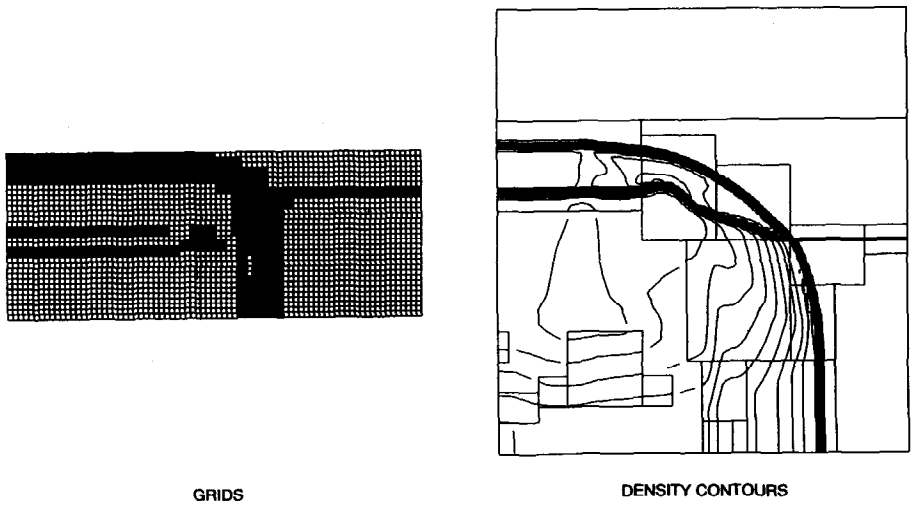

FIG. 20. Two-dimensional reactive Euler equations (5): Rate-stick problem by Roe's method, solution after 100 time steps.

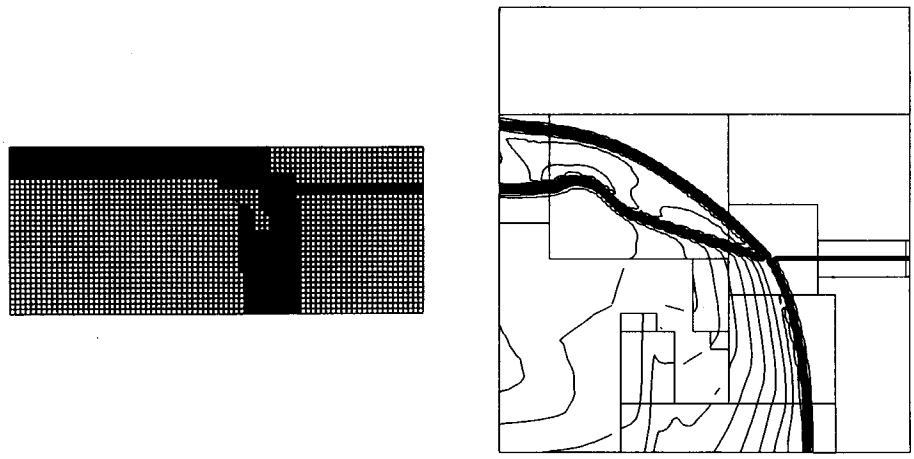

FIG. 21. Two-dimensional reactive Euler equations (5): Rate-stick problem by Roe's method, solution after 120 time steps.

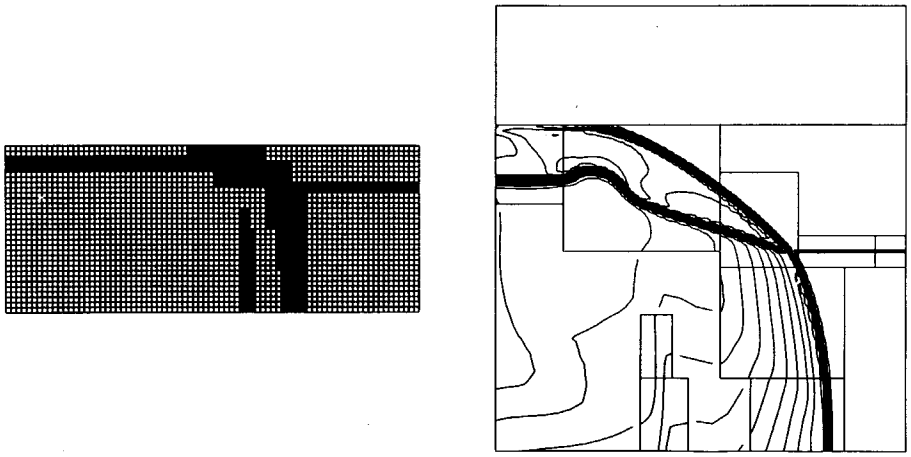

FIG. 22. Two-dimensional reactive Euler equations (5): Rate-stick problem by Roe's method, solution after 140 time steps.

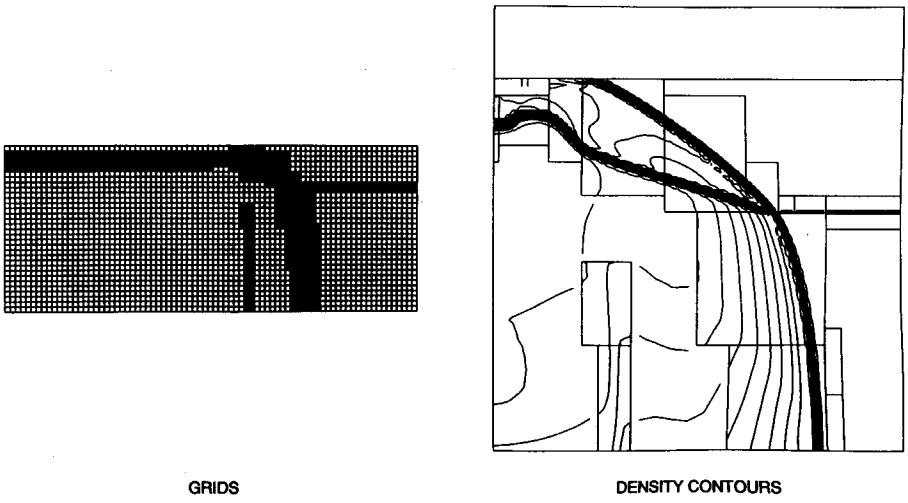

FIG. 23. Two-dimensional reactive Euler equations (5): Rate-stick problem by Roe's method, solution after 160 time steps.

problem. The solution is shown at intervals of 20 time steps. A strong shock front is developed followed by a reaction zone. At early times, the shock is one-dimensional along the central line (line of symmetry) and tends to curve near the interface between the reactant and the inert casing. This is a result of different propagation speeds in the different materials. Strong wave interaction is observed between the fully reacted material and the casing. The strong initial pressure gradient generates a strong shock wave that pushes the casing outwards. A strong expansion fan is observed which gradually penetrates the inner part of the reactive material. Grid motion, based on local density gradients, follows nicely the active flow regions. New fine patches are layed down as the flow develops, which are later removed when they are not required.

7. CONCLUDING REMARKS

Reactive flow problems make more demands on a computational method than inert flow problems. The difficulties arise partly from the fact that we have to resolve not just the shock waves but any associated reaction regions. Also the narrow spike that typifies detonation waves is very hard to capture.

We have examined, in a simple one-dimensional context, one classical scheme (MacCormack's) and five schemes designed for good discontinuity resolution: moving finite element (MFE), random choice (RCM), and a hybrid extension, a first-order Godunov method and a second-order Roe method. The MacCormack scheme was discarded because of the difficulty of equipping it with a suitable artificial viscosity. MFE worked beautifully on one problem, but in general did not provide enough control over the mesh to give reliable solutions. We could have used other moving mesh techniques, although in retrospect we feel that they are not as attractive as our actual choice. The

[redacted]

dimensional extensions. The first-order Godunov method did not provide sufficient resolution.

This left the second-order Roe scheme as the only viable candidate for further development, although most of the related high order Godunov methods would probably have served equally well. The linearisation of the Euler equations, extended to include mass fraction variables, is not difficult.

The spatial resolution needed for two-dimensional calculations was achieved by adaptive mesh refinement. Previous experience with inert problems suggests that this idea combines well with high-resolution upwind schemes because the upwinding provides accurate fluxes at the interface between fine and course grids. This experience was confirmed in the present case.

We obtained well-resolved results for the problem of a rate-stick detonated within a confining shell. These clearly reveal the distortion of the explosive/casing interface and the resulting weakening of the detonation wave. The chosen method seems capable of modelling a variety of events in both confined and unconfined explosives.

ACKNOWLEDGMENTS

The work described above was generously supported by AWE, Aldermaston, and RARDE, Fort Halstead. The authors thank Ian Cameron and David Rowse for many interesting and fruitful discussions.

REFERENCES

1. D. A. Anderson, J. C. Tannehill, and R. H. Pletcher, *Computational Fluid Mechanics and Heat Transfer* (Hemisphere, Washington, DC/New York, 1984).
2. M. Berger and P. Collela, *J. Comput. Phys.* **82**, 67 (1989).
3. J. B. Bdzil, *J. Fluid Mech.* **108**, 195 (1981).
4. A. Chorin, *J. Comput. Phys.* **22**, 517 (1976).
5. J. F. Clarke, P. L. Roe, L. G. Simmonds, and E. F. Toro, CoA Report 87/04. Cranfield Institute of Technology, Cranfield, UK, 1987 (unpublished).
6. P. Colella, *SIAM J. Sci. Stat. Comput.* **3**, 76 (1982).
7. M. G. Edwards, in *Proceedings, Seventh GAMM Conference*, edited by M. Deville (Vieweg, Brunswick, 1988), p. 72.
8. B. Einfeldt, CoA Report 8810, Cranfield Institute of Technology, Cranfield, UK, July 1988 (unpublished).
9. B. Einfeldt, C. D. Munz, P. L. Roe, and B. Sjögreen, "On Godunov Type Methods near Low Densities," 1989, preprint.
10. W. Fickett, "Detonation in Miniature," in *Mathematics of Combustion*, edited by J. D. Buckmaster (SIAM, Philadelphia, 1985), Chap. 4, p. 133.
11. W. Fickett and W. Davies, *Detonation* (Univ. of California Press, Berkeley, 1979).
13. S. K. Godunov, *Mat. Sb.* **47**, 271 (1959) [Russian]; also in *USJPRS Transl.* **7226**, 1960.
14. A. Harten, *J. Comput. Phys.* **49**, 357 (1983).
15. S. Karni, *SIAM J. Num. Anal.* **29**, 1592 (1992).
16. S. Karni, *J. Comput. Phys.*, submitted.
17. R. J. Leveque and H. C. Yee, *J. Comput. Phys.* **86**, 187 (1990).
18. R. W. MacCormack, AIAA Paper 69-354, 1969 (unpublished).
19. K. Miller and R. Miller, *SIAM J. Numer. Anal.* **18**, 1033 (1981).
20. S. Osher and J. A. Sethian, *J. Comput. Phys.* **79**, 12 (1988).
21. J. J. Quirk, CoA Report No. NFP 90/03, Cranfield Institute of Technology, Cranfield, UK, March 1990 (unpublished).
22. P. L. Roe, *J. Comput. Phys.* **43**, 357 (1981).
23. P. L. Roe, "Characteristic-Based Schemes for the Euler Equations," in *Ann. Rev. Fluid Mech.*, edited by M. van Dyke *et al.* (Annual Reviews Inc., Palo Alto, CA, 1986), Vol. 18, p. 337.

24. P. L. Roe, *Lecture Notes in Mathematics*, Vol. 1270, edited by Carasso *et al.* (Springer-Verlag, New York/Berlin, 1986).
25. H. B. Stewart and B. Wendroff, *J. Comput. Phys.* **56**, 363 (1984).
26. D. S. Stewart and J. B. Bdzil, *J. Fluid Mech.* **17**, 1 (1986).
27. P. K. Sweby, *Notes on Numerical Fluid Mechanics*, Vol. 24 (Vieweg, Brunswick, 1989), p. 599.
28. P. K. Sweby, *SIAM J. Num. Anal.* **21**, 995 (1984).
29. E. F. Toro and P. L. Roe, in *Proceedings, 16th International Symposium on Shock Tubes and Waves, Achen, Germany, 1987.*
30. J. C. T. Wang and G. F. Widophf, *Comput. Fluids* **18**, No. 1, 103 (1990).
31. H. C. Yee and J. L. Shinn, AIAA Paper 87-1116, 1987 (unpublished).